A computational study of homogeneous liquid–vapor nucleation in the Lennard-Jones fluid

Vincent K. Shen and Pablo G. Debenedetti[a)]
Department of Chemical Engineering, Princeton University, Princeton, New Jersey 08544

(Received 1 February 1999; accepted 26 May 1999)

Umbrella sampling Monte Carlo simulations are used to calculate free energy barriers to homogeneous liquid–vapor nucleation in the superheated Lennard-Jones fluid. The calculated free energy barriers decrease with increased superheating and vanish at the spinodal curve. A statistical geometric analysis reveals the existence of two types of voids: Small interstitial cavities, which are present even in the equilibrium liquid, and much larger cavities that develop as the system climbs the nucleation free energy barrier. The geometric analysis also shows that the average cavity size within the superheated liquid is a function of density but not of temperature. The critical nucleus for the liquid–vapor transition is found to be a large system-spanning cavity that grows as the free energy barrier is traversed. The weblike cavity is nonspherical at all superheatings studied here, suggesting a phenomenological picture quite different from that of classical nucleation theory. [S0021-9606(99)50232-8]

I. INTRODUCTION

Fundamental knowledge of the transformation of the liquid state of matter into the vapor phase is far from complete. Important questions remain, both about the molecular mechanisms that trigger the liquid–vapor transition, as well as on the rates at which these elementary processes occur.[1–3] This amounts to a significant gap in our present understanding of the liquid state, and one which limits our knowledge of phenomena as varied and important as cavitation erosion,[4] sonoluminescence,[5] explosive boiling,[6,7] and the mechanical strength of liquids.[8] In this paper, we report results of a computational investigation of the energetics and molecular mechanisms of the liquid–vapor transition; this work is part of an ongoing project aimed at improving our fundamental understanding of the rates and mechanisms of this basic phenomenon.

The formation of a vapor phase from a superheated liquid is an activated process, in which a free energy barrier must be overcome in order for the phase transition to occur. This is true for all first-order phase transitions, so long as the starting condition is metastable. Surmounting the free energy barrier amounts to the formation of a critically sized nucleus of the stable phase from within the bulk, metastable mother phase. Once the critical nuclei are formed, they grow spontaneously. Suspended impurities or container walls can provide interfaces that lower the free energy barrier to the formation of critical nuclei. In the absence of such pre-existing interfaces, the formation of critical nuclei occurs by a process known as homogeneous nucleation, a fundamental mechanism of first-order phase transitions. Classical nucleation theory[1–3,9] has traditionally provided a qualitative description of the nucleation process by treating nuclei of the stable phase thermodynamically and assuming that such objects are macroscopic in size. A basic goal of the theory is to calculate the nucleation rate, that is to say the rate at which critical nuclei are formed. This important quantity governs the attainable extent of penetration into the coexistence region. In general, the nucleation rate, J, can be written as

$$J = A \cdot \exp\left(\frac{-\Delta G}{k_B T} \right), \tag{1}$$

where J is the number of critical nuclei formed per unit time per unit volume; A is a kinetic factor which depends only weakly on temperature; ΔG is the free energy barrier to nucleation, that is to say the reversible work of formation of a critical nucleus; k_B is Boltzmann's constant; and T is the temperature. The calculation of J, therefore, entails a kinetic problem (determining A) and a thermodynamic one (determining ΔG). In this paper, we address the latter problem.

For the case of vapor to liquid nucleation, the free energy barrier, as predicted by the classical theory, is given by[10]

$$\Delta G = \frac{16\pi\gamma^3 v^2}{3 \cdot (\Delta\mu)^2}, \tag{2}$$

where γ is the interfacial free energy (surface tension), which is usually taken to be the same as that for an infinite planar interface; v is the specific volume in the liquid phase; and $\Delta\mu$ is the difference in chemical potential between the vapor and liquid phases at the given temperature and bulk pressure. The free energy barrier arises as a consequence of two competing effects. On the one side, the formation of the new phase requires the creation of an interface, which is an energetically unfavorable process. The second effect is the change in chemical potential that accompanies the phase transition, which is thermodynamically favorable. One of the

[a)]Electronic mail: pdebene@princeton.edu

crucial assumptions in the development of classical nucleation theory is that the fluid inside the nucleus behaves as if it were a uniform, bulk phase.

It is important to recall that the classical theory,[1–3,9] whose basic ideas underlie most discussions of nucleation, was originally developed explicitly for treating liquid droplet formation from supercooled vapors. Furthermore, its basic premise, namely that the critical nucleus is a macroscopic object amenable to thermodynamic treatment, applies only in the proximity of the phase coexistence boundary, that is to say for small degrees of penetration into the metastable regime. The conceptual picture is that liquidlike embryos are formed by local density fluctuations in a supersaturated vapor. Clusters of some critical size serve as nuclei around which the stable phase grows. The key idea is that clusters, or embryos, grow by sequential accretion of single molecules and shrink by single molecule depletion. In other words, embryos of the new phase serve as building blocks for the critical nucleus. In the case of nucleation in superheated liquids, the situation of interest here, key aspects of the above picture appear problematic. While it is easy to picture the formation of cavities by density fluctuations in a superheated liquid, the relation of such objects to critically sized bubbles formed by a sequential, single-molecule process is not obvious. Thus, the very notion of a spherical, macroscopic critical bubble formed by a succession of single-molecule events seems difficult to reconcile with actual processes occurring on a molecular scale.

Direct experimental tests of classical nucleation theory predictions have only been possible in the last fifteen years, thanks to the refinement of two techniques, the piston chamber[11] and the thermal diffusion cloud chamber,[12] to the point of allowing the accurate, direct measurement of nucleation rates. So far, this has only been done for droplet nucleation from supercooled vapors. These measurements demonstrate that the classical theory provides an accurate description of the isothermal dependence of the nucleation rate upon supersaturation, but fails to describe the temperature dependence.

From a theoretical perspective, the use of macroscopic and phenomenological arguments to aid in the description of an inherently microscopic process, as in the classical theory, leads to internal inconsistencies, several of which have been debated in the scientific literature[13–17] without, until recently,[18] satisfactory resolution. An important deficiency of the classical theory is its failure to predict any qualitative change in the behavior of a system as the depth of penetration into the metastable region is increased. In particular, the classical theory does not allow for loss of stability. This requires a detailed treatment of the structure and thermodynamics of the inhomogeneous interface between the embryo and the mother phase, first accomplished by van der Waals,[19] whose approach subsequently became the core of the Cahn–Hilliard theory.[20]

In recent years, there have been important advances in the theory of nucleation, mostly on the formation of a liquid phase from a supercooled vapor. McGraw and Laaksonen[21] have shown, using scaling arguments, that the difference between actual and classical barrier heights (reversible work of forming a critical nucleus) depends on temperature but not on supersaturation. This explains the experimental observations of nucleation rates[11,12] in supercooled vapors. These authors also showed that the classical theory provides very accurate predictions on the number of molecules in the critical nucleus, an important quantity that is amenable to measurement thanks to the so-called nucleation theorem.[22,23] The nucleation theorem is an exact relationship between the composition of the critical nucleus and the derivative of the free energy barrier, ΔG, with respect to the bulk-phase chemical potential of a component in the system. Measurements of the supersaturation dependencies of the nucleation rate[11,12] then yield, via Eq. (1) and independent knowledge of A, the composition of the critical nucleus.

Reiss and co-workers have developed the concept of a physically consistent cluster based on a precise definition of what constitutes a molecular cluster.[24–27] By doing this, the molecular configurations that contribute to the partition function of the inhomogeneous, supercooled vapor can be enumerated, allowing the free energy barrier to liquid droplet formation to be determined, although computer simulation is required to calculate this quantity.[24,25] In addition, these authors introduced a modified liquid drop theory that combines elements of the physically consistent cluster approach with the conventional capillarity approximation.[26] A kinetic theory based on the modified liquid droplet model[27] yields nucleation rates that have the same supersaturation dependence as the classical theory, but different temperature dependence, in agreement with experimental observation. Despite the significant theoretical advance that the physically consistent cluster approach represents, it is only applicable to dilute supercooled vapors.

The above advances have been limited to nucleation of liquids from vapors. A very important development that is not restricted to vapor–liquid nucleation is density functional theory. In this approach, pioneered by Oxtoby and co-workers,[28–33] one obtains the free energy barrier to nucleation by locating the stationary condition of the inhomogeneous grand potential with respect to the density profile across the interface between the bulk metastable phase and the nucleus of the stable phase. Although it is a continuum theory, the length scales over which this approach has been applied are microscopic. Calculations for bubble nucleation in stretched[29] liquids have shown that nonclassical effects are much more pronounced in bubble nucleation than in droplet nucleation. An important advantage of density-functional theory is that it predicts, correctly, a vanishing free energy barrier at the spinodal. However, the spherical nature of the critical nucleus is assumed at the outset, and this is an important limitation of the theory, especially at high superheatings.

Computer simulation has played an important role in furthering the fundamental understanding of the microscopic basis of nucleation and its eventual translation into a sound theoretical framework. Early Monte Carlo simulation studies investigated the free energies of liquidlike clusters.[34,35]

These studies, along with more recent simulations,[36] have clarified the notion of a physically consistent cluster. Modified microcanonical molecular dynamics has been used with some success to study vapor–liquid nucleation.[37,38] Recently, a simulation methodology based on linear response theory has been applied by Frenkel and co-workers to predict nucleation rates. Their approach consists of dividing the overall problem into a thermodynamic and a rate calculation. The thermodynamic calculation, whose purpose is to compute the free energy barrier to nucleation, consists of umbrella sampling Monte Carlo. It has been applied to crystal nucleation from supercooled liquids[39–42] and to liquid nucleation from supercooled vapors.[43–46] The thermodynamic calculation also leads to the identification of the critical nucleus. The kinetic part of the calculation involves performing molecular-dynamics simulations starting at the top of the free energy barrier and computing transmission coefficients.[41,42,46]

Just as nucleation theories have focused mainly on liquid droplet formation from supercooled vapors, so too have the majority of computer simulation studies. In particular, there have been few computational studies of homogeneous bubble nucleation.[29,47] Corti and Debenedetti studied the superheated Lennard-Jones fluid using the restricted and void-constrained ensembles.[48,49] These constrained simulations investigated the effect of restricting the magnitude of density fluctuations or the size of voids on the structure and thermodynamics of the superheated liquid, which was effectively prevented from phase-separating. In Ref. 48 umbrella sampling simulations were performed on small systems to examine the height of the free energy barrier and the transition from nucleation to spinodal decomposition. Together with subsequent studies,[50] showing the importance of investigating the statistics of fluctuating void space in the superheated liquid, these investigations[48–50] provide the basis of the present work.

In this paper, we investigate the free energy barriers to nucleation in the liquid–vapor transition in the Lennard-Jones fluid. We also apply a statistical geometrical analysis to study the voids and cavities that form in the superheated liquid. This work is part of an ongoing project aimed at improving our current understanding of the energetics, kinetics, and microscopic mechanisms of homogeneous nucleation in superheated liquids through molecular-based computer simulations. The paper is structured as follows. Section II explains the strategy to calculate free energy barriers, and the details of its implementation are given in Sec. III. Results are presented and discussed in Sec. IV. The main conclusions and suggestions for future work are presented in Sec. V.

II. UMBRELLA SAMPLING

In order to investigate free energy barriers to bubble nucleation, it is necessary to examine infrequently sampled, high-energy configurations. The technique used to accomplish this is umbrella sampling Monte Carlo, developed by Torrie and Valleau.[51]

Although fluctuations become more infrequent as the size of the system is increased, in umbrella sampling this problem is circumvented by biasing the system to sample rare fluctuations. However, the identification of the resulting free energy barrier with the work of formation of a single critical nucleus is a more subtle point, requiring in principle the formation of a well-defined nucleus in an otherwise unperturbed bulk. The present work represents a first step towards addressing this question for the liquid–vapor transition.

The basic idea can be illustrated, for the case of interest, by assuming that there exists an order parameter, Φ, that characterizes the evolution of a system as it changes from a superheated liquid to a vapor. Then, in the isothermal–isobaric (NPT) ensemble, the probability density of finding the system in a state with order parameter Φ^* is

$$P(\Phi^*)=\frac{\int dV \int d\mathbf{q}^N \delta[\Phi-\Phi^*]\cdot\exp\{-\beta[U(\mathbf{q}^N)+P_{\text{ext}}V]\}}{\int dV \int d\mathbf{q}^N \exp\{-\beta[U(\mathbf{q}^N)+P_{\text{ext}}V]\}}, \tag{3}$$

where $U(\mathbf{q}^N)$ is the potential energy of interaction between molecules in the system, P_{ext} is the applied external pressure, β is $(k_BT)^{-1}$, and $\delta(x)$ is the Dirac delta function. The integration in Eq. (3) is carried out over all possible values of system volume, V, and all possible values of molecular coordinates, $\mathbf{q}^N$. The Gibbs energy is given by

$$G=-\frac{1}{\beta}\ln Q_{\text{NPT}}, \tag{4}$$

where Q_{NPT} is the isothermal-isobaric partition function.[52] From this, it can be seen that the free energy can be expressed as a function of the order parameter, $G(\Phi)$

$$G(\Phi)=c-\frac{1}{\beta}\ln P(\Phi), \tag{5}$$

where c is a constant, whose value is not important for present purposes, since we are only concerned with free energy differences. The task of calculating $G(\Phi)$ reduces to the calculation of $P(\Phi)$, given in Eq. (3).

We note that $P(\Phi)$ is an equilibrium property of the system. If one were to use conventional Metropolis Monte Carlo[53] to calculate this probability distribution, one would find that the statistics so gathered are only successful in describing the system in its metastable superheated liquid phase and stable gas conditions, but not in the intermediate states traversed in going from a metastable to a stable condition. This is so because in the Metropolis algorithm, the probability of sampling high-energy configurations, being governed by the Boltzmann factor, is small, resulting in poor statistics for intermediate values of density, such as are of interest here. In order to sample high-energy configurations efficiently, we multiply and divide Eq. (3) by a biasing function, $\omega(\Phi)$

$$P(\Phi^*)=\frac{\int dV\int d\mathbf{q}^N\delta[\Phi-\Phi^*]\omega^{-1}(\Phi)\omega(\Phi)\exp\{-\beta[U(\mathbf{q}^N)+P_{\text{ext}}V]\}}{\int dV\int d\mathbf{q}^N\omega^{-1}(\Phi)\omega(\Phi)\exp\{-\beta[U(\mathbf{q}^N)+P_{\text{ext}}V]\}}. \tag{6}$$

Introducing $\omega(\Phi)$ allows one to calculate equilibrium properties while sampling from a non-Boltzmann probability distribution, $\omega(\Phi)\exp\{-\beta[U(\mathbf{q}^N)+P_{\text{ext}}V]\}$, no matter how unphysical the biased distribution might be. Essentially, one is simply biasing the simulation to explore infrequently sampled regions of phase space, and then correcting for the bias at the end. The correction that must be applied can be seen more clearly by expressing Eq. (6) in the following manner:

$$P(\Phi^*)=\frac{\left\langle\frac{\delta(\Phi-\Phi^*)}{\omega(\Phi)}\right\rangle_\omega}{\left\langle\frac{1}{\omega(\Phi)}\right\rangle_\omega}, \tag{7}$$

where the $\langle\ \rangle_\omega$ denotes average quantities as determined using the biased distribution. The biasing function is chosen so that sampling is performed within an order parameter window of width $\Delta\Phi$. Thus, a series of umbrella sampling runs are performed on several adjacent order parameter windows to obtain an entire free energy curve. The size of the sampling windows need not be uniform, and the windows can overlap if desired. Within each window, the relative free energy curve is calculated by Monte Carlo simulation and then curve-fitted to a polynomial in Φ. The free energy curves from adjacent windows are then ''linked'' by adjusting the value of the constant in the curve fit. One can think of this series of simulations as the computational equivalent of moving the system reversibly in order parameter space so that all of the important states in configuration space are well sampled as the phase transformation takes place.[54]

III. SIMULATION DETAILS

Nucleation experiments are normally conducted at constant pressure and temperature, and we have therefore chosen to conduct our calculations of free energy barriers in the NPT ensemble, fixing the pressure at the saturation pressure and varying the temperature to create superheating.

In order to estimate an adequate system size for the simulations, we invoke classical nucleation theory. Since the pressure in the critical nucleus is approximately equal to the vapor pressure at the bulk temperature,[55] we write, for the radius of the critical nucleus, r^*

$$r^*=\frac{2\gamma}{P_{\text{vp}}(T)-P}, \tag{8}$$

where P_{vp} is the vapor pressure at the given temperature, and P is the bulk pressure. This allows the determination of the size of a simulation box necessary to hold the critical nucleus. If one assumes bulk liquid conditions, then a conservative estimate for the system size can be made. These calculations are shown in Fig. 1, from which it follows that the higher the saturation temperature, the smaller the required system size, for a given supersaturation. The inset to Fig. 1 shows the conditions simulated in this work. The sample size was chosen to be 3500 Lennard-Jones atoms. This is the number of atoms that will hold a critical nucleus at 8.2% superheating, using a reduced saturation pressure ($P^*=P\sigma^3/\epsilon$) of 0.0463. Interactions were truncated beyond a distance equal to one-fifth of the simulation box length, and this truncation was compensated by using a long-range correction.[52] A vectorized version of a linked-cell list[52] was implemented to speed up the simulations.

The relevant order parameter that characterizes the system as it changes from liquid to vapor is the reduced number density, ρ, which can be conveniently expressed as follows:

$$\Phi\equiv\frac{\rho-\rho_{\text{liquid}}}{\rho_{\text{gas}}-\rho_{\text{liquid}}}, \tag{9}$$

where ρ_{liquid} and ρ_{gas} are the reduced number densities of the coexisting liquid and vapor phases at the saturation pressure ($\rho=N\sigma^3/V$). At the chosen saturation conditions, ρ_{liquid} and ρ_{gas} are 0.633 and 0.047 78, respectively. Φ ranges from zero in the liquid phase to unity in the vapor phase. Note that this is a global order parameter, and it does not specify anything *a priori* regarding the internal structure of the system.

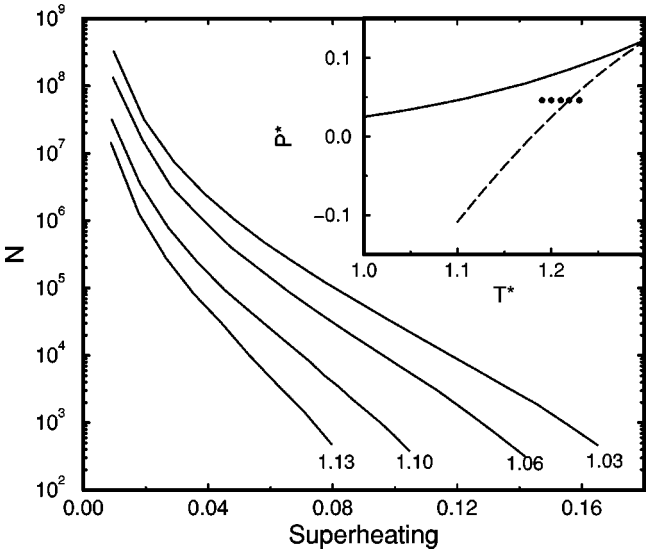

FIG. 1. Number of molecules in the simulation cell (N) required to accommodate one classical critical nucleus as a function of superheating, $(T_{\text{sim}}-T_{\text{sat}})/T_{\text{sat}}$, where T_{sim} is the simulation temperature and T_{sat} is the saturation temperature at the given pressure. Surface tension data of Abbas and Nordholm (Ref. 65) were used in conjunction with Eq. (8) to perform the calculation. The labels on the curves correspond to different temperatures, expressed in units of ϵ/k_B, where ϵ is the Lennard-Jones energy and k_B is Boltzmann's constant. The inset shows the state conditions simulated in this work (●), corresponding to a pressure $P^*=0.0463$. Also shown are the calculated binodal (—) and superheated liquid spinodal (– – –) for the Lennard-Jones fluid (Ref. 56). Pressure is given in units of ϵ/σ^3, and temperature is given in units of ϵ/k_B.

Local order parameters have been used in free energy barrier calculations of liquid droplet and crystal nucleation.[41–46] They have the advantage of providing an unambiguous interpretation of the free energy barrier as the reversible work needed to form a *single* critical nucleus. Corti and Debenedetti[49] used a local and quantitative measure of void space in their study of the superheated Lennard-Jones fluid. They measured the largest sphere that could be inserted in a void without overlapping with the surrounding atoms. Work is in progress on the efficient implementation of this type of local order parameter for the bubble nucleation problem, in particular on its generalization from voids to bubbles. Here, we report on umbrella sampling simulations that employ the bulk density as a global order parameter, and we present a possible local order parameter definition in Sec. V.

Within each order parameter sampling window, the umbrella sampling simulations were conducted as follows. We define a sampling window as $\Phi^* \pm (\Delta\Phi/2)$. For each sampling window, an initial random configuration corresponding to Φ^* was generated. Each configuration was then equilibrated for 2500 MC cycles. One cycle in the equilibration period consisted of each molecule being subjected to a trial move. The percentage of accepted molecule moves was maintained at ~50%. Statistics were then gathered over 35 000 MC cycles, in which volume displacements were conducted with the same probability as molecule displacements. In the production portion of the simulation, one cycle consisted of N trial molecule displacements and N trial volume displacements, where N is the number of molecules in the system. The percentage of accepted atom displacements was maintained at ~50%, while the percentage of accepted volume displacements was maintained at ~75% to obtain sufficient statistics within the order parameter sampling window. The relative free energy curves from each sampling window were fitted to third degree polynomials and the constant in the polynomial adjusted such that curves from adjacent windows fitted smoothly.

The biasing function, $\omega(\Phi)$, was chosen to be of the following form within each sampling window:

$$\omega(\Phi) = \exp\{a - b(\Phi_{\max} - \Phi)^2\}. \tag{10}$$

The logarithm of Eq. (10) is a parabola, which we demand to be concave down. $\Phi_{\max}$ is the location of the parabola's maximum, b adjusts the width of the sampling window, and a is a constant, whose value is chosen for numerical convenience. Adjustment of b and $\Phi_{\max}$ biases the simulation to preferentially sample configurations within the desired order parameter window.

In the following section, we present simulation results that are in satisfying agreement with expected thermodynamic trends, such as a decreasing free energy barrier with increasing temperature, and stability loss in the spinodal region. Relatively large system sizes (3500) were employed to this end. However, because the simulations use a global order parameter, both the sample size dependence of the calculated free energy barriers and their difference, if any, with respect to values obtained using a local order parameter need to be investigated systematically. Work is in progress on both these questions.

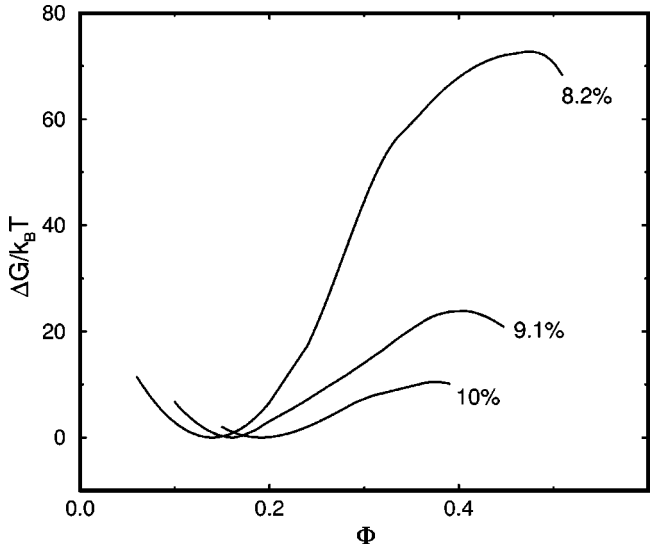

FIG. 2. Free energy curves calculated by umbrella sampling for the Lennard-Jones fluid at superheatings, $(T-T_{\text{sat}})/T_{\text{sat}}$, of 8.2%, 9.1%, and 10.0%. The x axis is the bulk density order parameter, defined in Eq. (9); it equals zero for the saturated liquid and is unity for the saturated vapor.

IV. RESULTS AND DISCUSSION

As shown in the inset to Fig. 1, free energy barrier calculations were performed at five different temperatures, or superheatings, at a fixed external pressure $P^* = 0.0463$. The calculated free energy curves at 8.2%, 9.1%, and 10% superheating are shown in Fig. 2. The location of the free energy minimum and maximum for each curve is given in Table I, as are the calculated values of the free energy barrier from simulation and classical theory. In a simulation, the free energy barrier is simply the free energy difference between the maximum and the minimum along a constant superheating curve. The free energy minima in Fig. 2 are only local metastable minima, the global minimum being located at $\Phi = 1$, which corresponds to the gas phase. Using the equation of state of Johnson *et al.*,[56] we have verified that the density corresponding to the local free energy minimum is the density of the liquid at the given pressure and temperature. It can be seen from Table I and Fig. 2 that the free energy barrier to nucleation decreases as the thermodynamic driving force (superheating) increases. Furthermore, the local free energy minimum shifts towards lower densities upon increased superheating, reflecting the fact that the liquid's density decreases upon isobaric heating. Both of these trends are in accord with thermodynamic expectations. At present, it is not possible to tell whether the agreement with classical

TABLE I. Summary of umbrella sampling results.

$(T-T_{\text{sat}})/T_{\text{sat}}$	$\Phi_{\min}$	$\Phi_{\max}$	$\Delta G_{\text{slm}}/kT$	$\Delta G_{\text{class}}/kT$
8.2%	0.140	0.470	72.7	73
9.1%	0.161	0.405	24	37
10.0%	0.191	0.376	10.5	21

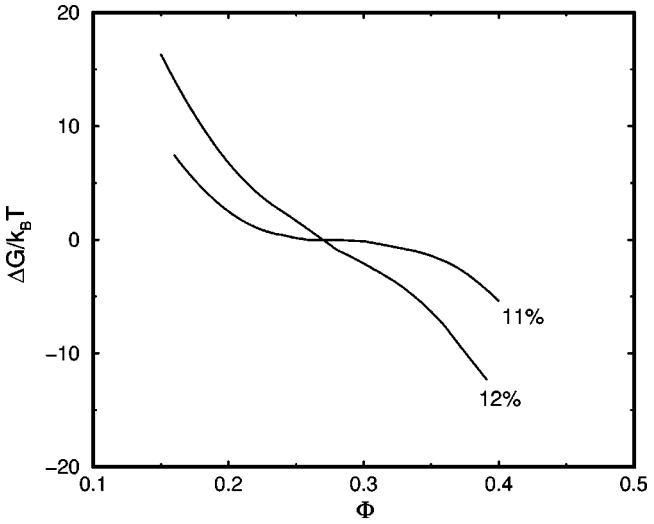

FIG. 3. Free energy curves calculated by umbrella sampling for the Lennard-Jones fluid within the unstable region (12% superheating), and at a limit of stability (Ref. 56) (11% superheating).

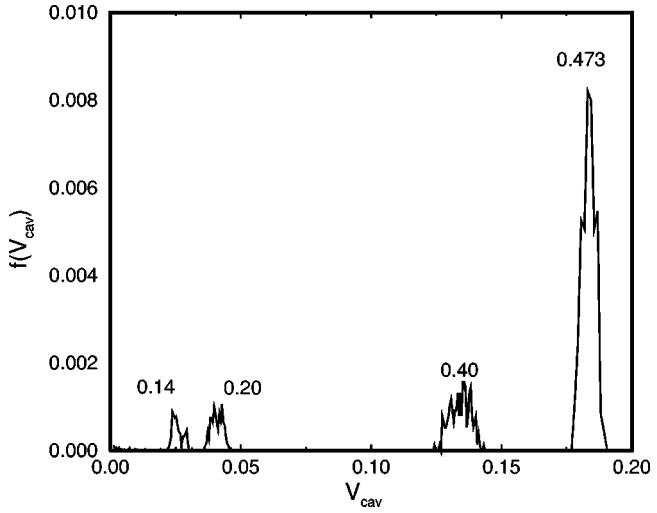

FIG. 4. Cavity size distributions at 8.2% superheating at various values of the order parameter. $f(V_{cav})$ is the fraction of the total number of cavities of size V_{cav}. V_{cav} is the volume fraction of the simulation box at the given density. A bin size of 5.0×10^{-5} in volume fraction units was used to calculate these distributions.

theory at 8.2% superheating signals the attainment of asymptotic convergence close to coexistence, or whether it represents the crossing of two curves. Elucidation of this question requires simulations closer to coexistence, and hence much larger sample sizes (Fig. 1). Work is in progress on the parallelization of our code to handle larger systems.

One of the important limitations of classical nucleation theory is that it predicts a positive free energy barrier at the spinodal. Theories that appropriately take into account the nonuniform nature of the interface between the embryo and the bulk metastable fluid, on the other hand, correctly distinguish between unstable and metastable states. Examples of this are density functional theory and the van der Waals–Cahn–Hilliard theory of interfaces.[19,20] In order to study the behavior of the free energy barrier at large superheatings, we first performed umbrella sampling simulations at a temperature in the unstable region of the Lennard-Jones liquid, using a superheating of 12%. As shown in Fig. 3, there is no free energy barrier under these conditions. This is consistent with the fact that within the unstable region the phase transition occurs by spinodal decomposition, that is to say, by the spontaneous growth of density fluctuations exceeding a critical wavelength. No barrier crossing is required in this case.

Using the Johnson *et al.*[56] equation of state, the spinodal temperature at the given pressure was determined, and was found to correspond to 11% superheating. The free energy curve for the system at this condition is also shown in Fig. 3. The inflection is consistent with the system reaching a stability limit. Comparison of the free energy profiles at 10%, 11%, and 12% superheating (Figs. 2 and 3) shows that there is a transition from metastability to instability around 11% superheating. In reality, the transition from metastability to instability occurs over a narrow range of superheatings,[57–59] the spinodal being a useful idealization that becomes exact in the limit of infinitely long-ranged interactions. A precise location of this transition region by molecular simulation is difficult because the correlation length becomes very large in this region, and calculations such as the present one become unreliable because of finite size effects. We simply note that the agreement between the umbrella sampling calculations and the prediction of the empirical but accurate equation of state of Johnson *et al.*[56] is very good.

Umbrella sampling allows not only the thermodynamics of homogeneous nucleation to be studied, but also the nature of the pre-critical and critical structures that develop as the system climbs the free energy barrier. This is done by generating configurations during the course of umbrella sampling runs for subsequent analysis. This type of analysis has been done for vapor–liquid and liquid–solid nucleation,[39–46] but to our knowledge not for liquid–vapor nucleation. The relevant structures of interest here are low-density regions that eventually grow to form a critical nucleus of the vapor phase. To search for such low-density regions, we focus our attention here on cavities, which we define to be connected clusters of voids. Voids are defined to be the empty space not contained within the exclusion spheres of any atom in the system. We took the radius of an atom's exclusion sphere to be the Lennard-Jones σ. To study cavities, we implemented our recent void analysis algorithm,[60] which not only identifies individual cavities, but also calculates exactly the volume of each cavity in any configuration of N monodisperse spheres. The reader is referred to the original paper by Sastry *et al.*[60] for details. We simply note here that the identification of individual voids involves, as a initial step, a dual Voronoi–Delaunay tessellation, applied to each configuration of interest.

We first examined the distribution of cavity volumes for the Lennard-Jones fluid at various densities (order parameter windows) at 8.2% superheating, as shown in Fig. 4. The two extreme densities shown represent the system at its metastable free energy minimum ($\Phi=0.14$), and at the top of the free energy barrier ($\Phi=0.473$). The x axis gives the cavity volume normalized by the simulation cell's volume. The y axis gives the fraction of cavities with the given volume. For each reduced density, the number of cavities within a given

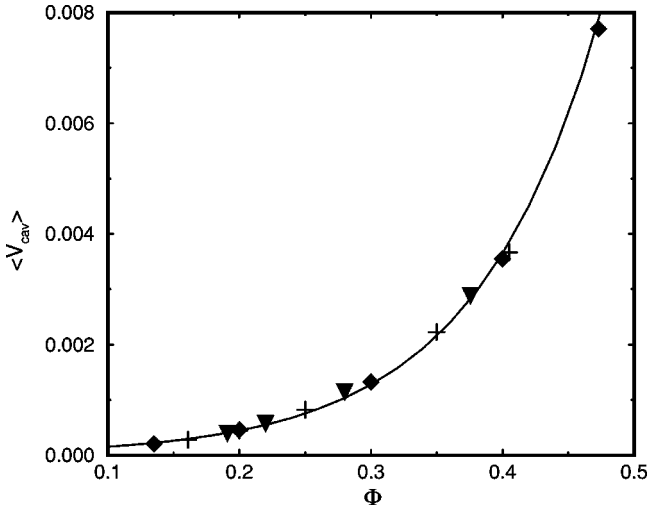

FIG. 5. Average cavity volume, $\langle V_{cav} \rangle$, as a function of the order parameter (reduced density) at three different superheatings, 8.2% ($\diamond$), 9.1% ($+$), and 10.0% ($\triangledown$). Note that all points fall on the solid line, an exponential fit of the data.

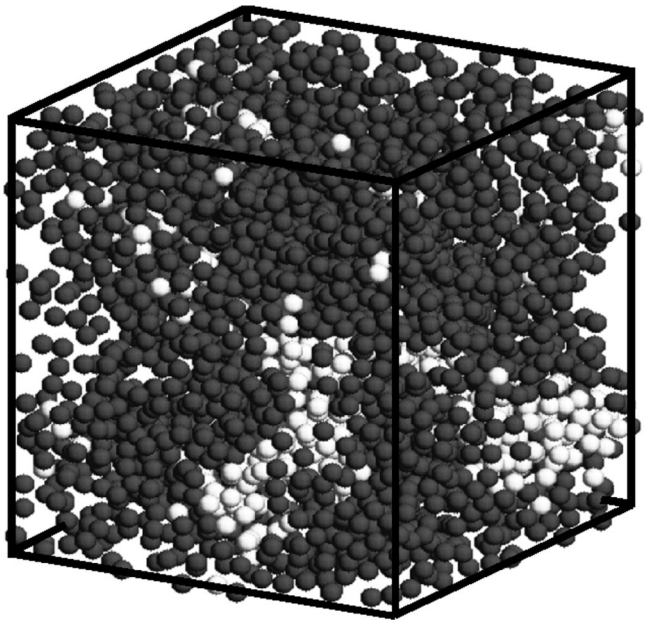

FIG. 6. Cavity (dark) and bulk (light) atoms corresponding to an umbrella sampling configuration at the top of the free energy barrier, at a superheating of 10%.

size range was counted in 200 configurations, and the distribution was then normalized by the total number of cavities found in each set of configurations. We chose our cavity volume bin size to be 5×10^{-5} in volume fraction units. Not shown in Fig. 4 is a large single peak, approaching unity at the smallest volume fraction. This feature was observed at all densities, including the saturated liquid and the metastable liquid at the minimum of the free energy barrier (Fig. 2). It corresponds to interstitial, not connected, voids. There is a fine structure within this ''peak,'' and voids can be found with volume fractions as low as 10^{-12}. However, we have omitted this from Fig. 4 because this feature does not change as the superheated liquid climbs the free energy barrier; it represents a ''background'' of interstitial voids that is present at all densities.

Figure 4 clearly shows that as the system climbs the free energy barrier, a large void space begins to appear. This void space takes the form of a single cavity that spans the entire system. At each reduced density, there is a finite range of sizes that this single cavity can take, as shown in Fig. 4. We found no cavities of intermediate sizes lying between the system-spanning and interstitial extremes. The size of this dominating cavity increases as the free energy barrier is climbed and the bulk density decreases. This trend is in accord with physical intuition, and it is this cavity that serves as the pre-critical and critical nucleus for the phase transition.

For each cavity size distribution curve, or equivalently, for each reduced density shown in Fig. 4, we calculated the average cavity volume at 8.2% superheating. The average cavity volume was calculated by determining the total cavity volume in each set of 200 configurations generated at each reduced density, and dividing by the total number of cavities (including the interstitial voids) found in the set of configurations. This average cavity volume is shown in Fig. 5 as a function of reduced density together with similar calculations for 9.1% and 10.0% superheating. We find that average cavity volumes at the three superheatings fall on the same curve, an exponential function of the order parameter, indicating that the mean cavity volume is a function of density only. The average cavity volume, in other words, is determined solely by geometry. A similar result was found by Sastry *et al.*,[61] for the free volume in the hard sphere fluid. In that work, the free volume was defined as the volume of the cavity that results when a hard sphere is removed from a given configuration. While statistical geometry and thermodynamics are one and the same thing for hard spheres, it is surprising to find a similar result for the Lennard-Jones fluid. The expectation is, therefore, that the influence of temperature, that is to say the deviation from purely geometric behavior, should manifest itself in the higher moments of the cavity volume distribution. Work is in progress on this aspect of the problem.

It has already been mentioned that there exists a large cavity that grows as the system climbs the free energy barrier. At the top of the free energy barrier, this cavity should be the critical nucleus for the liquid-vapor transition, and it is thus of great interest to examine its salient characteristics, which we show in two complementary ways.[62] The first approach is to identify Lennard-Jones particles as either cavity or bulk atoms. The former are those atoms whose Delaunay simplex contains a Voronoi vertex that lies within the cavity region.[60] In short, we identify those atoms that are associated with the large cavity and those atoms that are not. This is shown in Fig. 6, where the dark atoms are associated with the single system-spanning cavity, as identified by the algorithm (periodic boundary conditions were used). The light-shaded atoms are bulk atoms. We note that the configuration in Fig. 6 corresponds to a system at 10% superheating at the top of the free energy barrier, which should contain the smallest critical nucleus of all the simulations conducted in the metastable region. Alternatively, we can show the actual

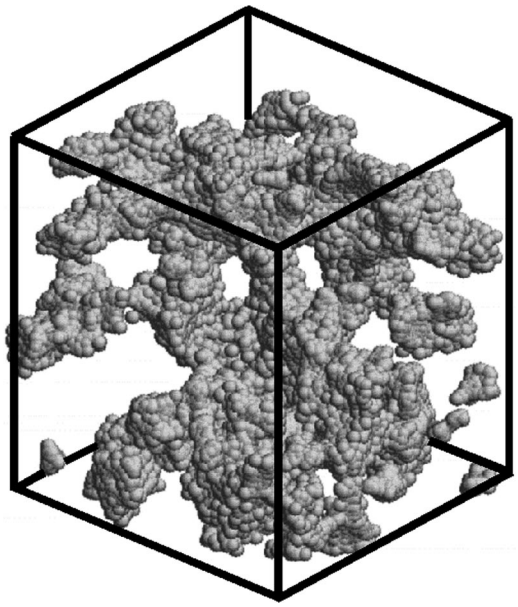

FIG. 7. Central portion of the system-spanning cavity at the top of the free energy barrier, at 10% superheating. This was obtained from the molecular configuration presented in Fig. 6. This cavity region was identified by first locating Voronoi vertices that lie in the cavity. The cavity space was then filled in by shooting spheres of radius 0.005σ randomly around the Voronoi vertices. The actual atoms have been removed from the picture. Side length of depicted cube is 0.3 of simulation box.

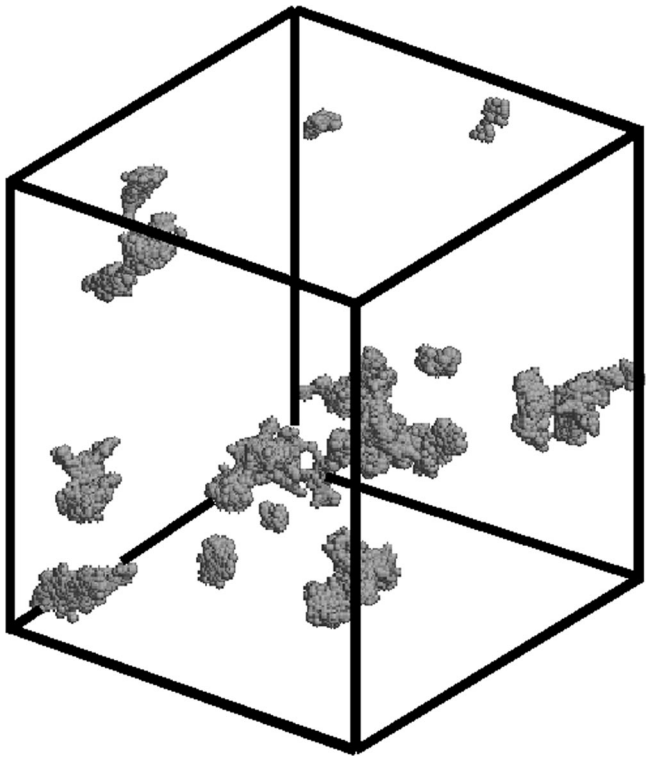

FIG. 8. Cavity pockets in the equilibrium Lennard-Jones liquid at saturation ($P^*=0.0463$, $T^*=1.10$). Different cavities are denoted by different shadings. Periodic boundary conditions are used. Full simulation box shown; actual atoms removed for clarity.

cavity and remove the atoms. This is done in Fig. 7, which shows only the central portion of the system-spanning cavity. It is clear that there exists a weblike cavity network that percolates throughout the system. This type of cavity also exists for configurations at the top of the free energy barrier at other superheatings, including 8.2%, which is as close to coexistence as we can currently simulate. These cavities are far from spherical, in all cases, and this represents a marked deviation from the picture assumed in classical nucleation theory.

For completeness, we show the cavities that exist in the equilibrium liquid in Fig. 8. In the stable, equilibrium liquid, there is no cavity network, but several small, separate cavity pockets. These cavities grow and coalesce to form a large weblike cavity as the system climbs the free energy barrier. Thus, it might be possible to think of the process of precritical bubble growth in terms of the sequential accretion of individual *cavities* in analogy to the classical liquid drop model. Although this parallelism might seem attractive, the weblike character of the nonspherical cavity network is more indicative of pervasive loss of cohesion during the course of the liquid–vapor phase change. This is quite surprising, in that we have simulated a liquid under positive external pressure, and we must therefore conclude that the cavity-based analysis reveals a picture quite at odds with classical nucleation theory.

V. SUMMARY

We have shown that umbrella sampling is a convenient method for calculating free energy barriers to homogeneous nucleation of a vapor phase from a superheated liquid. For a system of 3500 Lennard-Jones atoms, umbrella sampling Monte Carlo simulations provide results that are in agreement with the expected thermodynamic trends. In particular, we find that the height of the free energy barrier to nucleation and the density of the bulk superheated liquid decrease upon isobaric heating. In addition, the technique predicts, correctly, the vanishing of the free energy barrier to nucleation upon sufficiently deep superheating, in contrast to the classical nucleation picture.

A geometric analysis reveals that in the equilibrium liquid there is a large population of small interstitial voids that are formed by local density fluctuations, along with fewer and larger cavity pockets. In the metastable, superheated Lennard-Jones liquid, we find a system-spanning, weblike cavity that grows in size as the superheated liquid climbs the free energy barrier. This large cavity is formed by the coalescence of small interstitial voids and cavity pockets. The conceptual picture that appears to emerge from the cavity analysis is one in which the liquid ''tears itself apart'' as the liquid–vapor transition takes place. This is rather different from the classical picture of spherical bubbles as critical nuclei. Our work, as well as the recent interesting study of cavities in supercritical water,[63] point to the useful insights into fluid structure than can result from a statistical geometric analysis of fluctuating void space.

Work is currently in progress on simulations with larger systems. This will allow for the investigation of the sample-size dependence of the calculated free energy barriers, as well as of the large cavities, which scaling arguments[21] suggest should reach an asymptotic size. We are also planning to study the rate of nucleation.[41] The approach which we have

taken so far involves the use of a global order parameter, namely density. While this seems a natural choice for liquid–vapor nucleation, we also plan to investigate the use of more local definitions of the order parameter. Finally, we note that our geometric analysis of structure has focused exclusively on cavities, which are empty regions of space, devoid, by definition, of any molecules. In reality, of course, a bubble contains molecules, and thus, one must accordingly look for low-density structures, not just voids.

A possible local order parameter for the liquid–vapor transition that reconciles the conceptual discrepancy between cavities and bubbles is the mean-squared distance between a given molecule i and its n nearest neighbors

$$\Phi_{\text{local}} \equiv \frac{1}{n}\sum_{j=1}^{n} r_{ij}^2. \tag{11}$$

The advantage of this local order parameter is that it allows for the presence of molecules within the developing vapor embryo. At the same time, no geometric shape is imposed *a priori* upon the nucleating phase. However, the choice of n, the number of nearest neighbors, requires some investigation. Our preliminary studies take the value of n to be sixteen.[64] At 10% superheating and for 3500 atoms, we calculated a free energy barrier height ($\Delta G/kT$) of 13.6. Under the same conditions and using the global order parameter, a free energy barrier height of 10.5 was calculated. The system size dependence of the difference between these two types of free energy barriers will be studied systematically in future work. We note here that preliminary cavity analysis of configurations at the top of the free energy barrier for the local order parameter calculations also show a system-spanning cavity, which includes the low density, bubblelike region defined by the local order parameter. More comprehensive studies utilizing this order parameter will be the subject of future communications.

ACKNOWLEDGMENTS

The financial support of the U. S. Department of Energy, Division of Chemical Sciences, Office of Basic Energy Sciences (Grant No. DE-FG02-87ER13714), and of the donors of the Petroleum Research Fund, administered by the American Chemical Society, is gratefully acknowledged.

[1] F. Abraham, *Homogeneous Nucleation* (Academic, New York, 1974).
[2] W. Döring, Z. Phys. Chem. (Leipzig) **36**, 37 (1937).
[3] J. Frenkel, *Kinetic Theory of Liquids* (Dover, New York, 1955).
[4] D. H. Trevena, *Cavitation and Tension in Liquids* (Adam Hilger, Bristol, 1987).
[5] D. F. Gaitan, L. A. Crum, R. A. Roy, and C. C. Church, J. Acoust. Soc. Am. **91**, 3166 (1992).
[6] R. C. Reid, Am. Sci. **64**, 146 (1976).
[7] R. C. Reid, Adv. Chem. Eng. **12**, 105 (1983).
[8] G. S. Kell, Am. J. Phys. **51**, 1038 (1983).
[9] R. Becker and W. Döring, Ann. Phys. (Leipzig) **24**, 719 (1935).
[10] P. G. Debenedetti, *Metastable Liquids* (Princeton University Press, Princeton, NJ, 1996).
[11] P. E. Wagner and R. Strey, J. Chem. Phys. **80**, 5266 (1984).
[12] C.-H. Hung, M. J. Krasnopoler, and J. L. Katz, J. Chem. Phys. **90**, 1856 (1989).
[13] J. Lothe and G. M. Pound, J. Chem. Phys. **36**, 2080 (1962).
[14] H. Reiss, J. L. Katz, and E. R. Cohen, J. Chem. Phys. **48**, 5553 (1968).
[15] M. Blander and J. L. Katz, J. Stat. Phys. **4**, 55 (1972).
[16] S. L. Girshick and C. P. Chiu, J. Chem. Phys. **93**, 1273 (1990).
[17] C. L. Weakliem and H. Reiss, J. Phys. Chem. **98**, 6408 (1994).
[18] H. Reiss, W. K. Kegel, and J. L. Katz, Phys. Rev. Lett. **78**, 4506 (1997).
[19] J. van der Waals, Verhand.Konink.Akad.Wetensch.Amsterdam Sect.1., Deel I, 2 (1893).
[20] J. W. Cahn and J. E. Hilliard, J. Chem. Phys. **31**, 688 (1959).
[21] R. McGraw and A. Laaksonen, Phys. Rev. Lett. **76**, 2754 (1996).
[22] D. Kashchiev, J. Chem. Phys. **76**, 5098 (1982).
[23] D. W. Oxtoby and D. Kashchiev, J. Chem. Phys. **100**, 7665 (1994).
[24] H. M. Ellerby, C. L. Weakliem, and H. Reiss, J. Chem. Phys. **95**, 9209 (1991).
[25] H. M. Ellerby and H. Reiss, J. Chem. Phys. **97**, 5766 (1992).
[26] C. L. Weakliem and H. Reiss, J. Chem. Phys. **99**, 5374 (1993).
[27] C. L. Weakliem and H. Reiss, J. Chem. Phys. **101**, 2398 (1994).
[28] D. W. Oxtoby and R. Evans, J. Chem. Phys. **89**, 7521 (1988).
[29] X. C. Zeng and D. W. Oxtoby, J. Chem. Phys. **94**, 4472 (1991).
[30] Y. C. Shen and D. W. Oxtoby, J. Chem. Phys. **104**, 4233 (1996).
[31] Y. C. Shen and D. W. Oxtoby, J. Phys.: Condens. Matter **8**, 9657 (1996).
[32] D. W. Oxtoby, Acc. Chem. Res. **31**, 91 (1998).
[33] C. Seok and D. W. Oxtoby, J. Chem. Phys. **109**, 7982 (1998).
[34] J. K. Lee, J. A. Barker, and F. F. Abraham, J. Chem. Phys. **58**, 3166 (1973).
[35] M. Rao, B. J. Berne, and M. H. Kalos, J. Chem. Phys. **68**, 1325 (1978).
[36] I. Kusaka, Z. G. Wang, and J. H. Seinfeld, J. Chem. Phys. **108**, 3416 (1998).
[37] K. Yasuoka and M. Matsumoto, J. Chem. Phys. **109**, 8451 (1998).
[38] K. Yasuoka and M. Matsumoto, J. Chem. Phys. **109**, 8463 (1998).
[39] J. S. van Duijneveldt and D. Frenkel, J. Chem. Phys. **96**, 4655 (1992).
[40] P. R. ten Wolde, M. J. Ruiz-Montero, D. Frenkel, Phys. Rev. Lett. **75**, 2714 (1995).
[41] P. R. ten Wolde, M. J. Ruiz-Montero, and D. Frenkel, Faraday Discuss. **104**, 93 (1996).
[42] P. R. ten Wolde, M. J. Ruiz-Montero, and D. Frenkel, J. Chem. Phys. **104**, 9932 (1996).
[43] P. R. ten Wolde, D. W. Oxtoby, and D. Frenkel, Phys. Rev. Lett. **81**, 3695 (1998).
[44] P. R. ten Wolde and D. Frenkel, J. Chem. Phys. **109**, 9901 (1998).
[45] P. R. ten Wolde and D. Frenkel, J. Chem. Phys. **109**, 9919 (1998).
[46] P. R. ten Wolde, M. J. Ruiz-Montero, and D. Frenkel, J. Chem. Phys. **110**, 1591 (1999).
[47] T. Kinjo and M. Matsumoto, Fluid Phase Equilibria **144**, 343 (1998).
[48] D. S. Corti and P. G. Debenedetti, Chem. Eng. Sci. **49**, 2717 (1994).
[49] D. S.Corti and P. G. Debenedetti, Ind. Eng. Chem. Res. **34**, 3573 (1995).
[50] S. Sastry, P. G. Debenedetti, and F. H. Stillinger, Phys. Rev. E **56**, 5533 (1997).
[51] G. M. Torrie and J. P. Valleau, Chem. Phys. Lett. **28**, 578 (1974).
[52] M. P. Allen and D. J. Tildesley, *Computer Simulation of Liquids* (Clarendon, Oxford, 1989).
[53] N. Metropolis, A. W. Rosenbluth, M. N. Rosenbluth, A. H. Teller, and E. Teller, J. Chem. Phys. **21**, 1087 (1953).
[54] D. Chandler, *Introduction to Modern Statistical Mechanics* (Oxford University Press, New York, 1987).
[55] Y. Kagan, Russ. J. Phys. Chem. **34**, 42 (1960).
[56] J. K. Johnson, J. A. Zollweg, and K. E. Gubbins, Mol. Phys. **78**, 591 (1993).
[57] C. Unger and W. Klein, Phys. Rev. B **29**, 2698 (1984).
[58] K. Binder, Phys. Rev. A **29**, 341 (1984).
[59] K. Binder, Physica A **140**, 35 (1986).
[60] S. Sastry, D. S. Corti, P. G. Debenedetti, and F. H. Stillinger, Phys. Rev. E **56**, 5524 (1997).
[61] S. Sastry, T. M. Truskett, P. G. Debenedetti, S. Torquato, and F. H. Stillinger, Mol. Phys. **95**, 289 (1998); P. G. Debenedetti and T. M. Truskett, Fluid Phase Equilibria **158-160**, 549 (1999).
[62] Pictures were generated with the aid of a program called RasMol developed by Dr. R. Sayle.
[63] R. D. Mountain, J. Chem. Phys. **110**, 2109 (1999).
[64] J. L. Meijering, Philips Res. Rep. **8**, 270 (1953).
[65] S. Abbas and S. Nordholm, J. Colloid Interface Sci. **166**, 481 (1994).